10
2-14

2048

MASTER

LA-4852-MS

AN INFORMAL REPORT

Resonant Absorption of Laser Light by Plasma Targets

los alamos
scientific laboratory
of the University of California
LOS ALAMOS, NEW MEXICO 87544

UNITED STATES
ATOMIC ENERGY COMMISSION
CONTRACT W-7405-ENG. 36

Printed in the United States of America. Available from
National Technical Information Service
U. S. Department of Commerce
5285 Port Royal Road
Springfield, Virginia 22151
Price: Printed Copy $3.00; Microfiche $0.95

LA-4852-MS
An Informal Report
UC-20

ISSUED: December 1971

los alamos
scientific laboratory
of the University of California
LOS ALAMOS, NEW MEXICO 87544

Resonant Absorption of Laser Light by Plasma Targets

by

J. P. Freidberg
R. W. Mitchell
R. L. Morse
L. I. Rudsinski

RESONANT ABSORPTION OF LASER LIGHT BY PLASMA TARGETS

by

J. P. Freidberg, R. W. Mitchell, R. L. Morse and L. I. Rudsinski

ABSTRACT

It is proposed that a resonant mechanism should cause significant absorption of energy from intense laser pulses in plasma targets, and that the energy should be deposited in such a way as to form a very non-Maxwellian high temperature tail on the electron velocity distribution.

Current interest in the controlled release of nuclear energy from laser-heated pellets of thermonuclear fuel has drawn interest to mechanisms by which laser light might be absorbed in the surface of such pellets. The large pulsed light intensities which are required for this heating and are beginning to be available in absorption experiments put the interaction of the laser radiation with the initially solid target in the approximately collisionless regime. Binary collisions between electrons driven by the wave fields and ions (sometimes called inverse bremstrahlung) can cause some absorption and may be quite important in allowing a weak precursor of a pulse to ionize the target and give the surface some thickness as assumed below, but as the intensity increases the fraction of the light energy absorbed by collisions becomes smaller.

In this letter we propose a resonant, collisionless absorption mechanism by which an inhomogeneous target plasma can absorb a significant fraction of obliquely incident laser light. We then show from numerical simulations that the energy is deposited in a very non-Maxwellian tail of the electron velocity distribution. Preliminary work on a relativistic absorption mechanism is also mentioned. If the electron density of the plasma, n_e, and therefore the dielectric constant, ϵ, are functions only of x, the light is incident with the wave vector $\bar{k}$ in the x,y plane at an angle θ to the x axis, and the $\bar{E}$ field is polarized in this plane, then the c.w. wave equation for the only nonzero component of the magnetic field, B_z, is

$$\frac{d^2B_z(x)}{dx^2} - \frac{1}{\epsilon(x)}\frac{d\epsilon}{dx}\frac{dB_z(x)}{dx} + k_o^2(\epsilon - \sin^2\theta)B_z(x) = 0 \qquad (1)$$

where $k_o = \omega/c$ is the free space wave number, $B_z(x,y,t) = B_z(x)\exp[-i\omega t + ik_y y]$ and $k_y = k_o \sin\theta$. Consider the familiar dielectric constant for a cold plasma with a collision frequency ν;

$$\epsilon(x) \simeq 1 - \frac{\omega_{pe}^2(x)}{\omega^2}\left(1 + \frac{i\nu}{\omega}\right) , \qquad (2)$$

where $\omega_{pe} = (4\pi n_e e^2/m_e)^{\frac{1}{2}}$ is the electron plasma frequency. In the collisionless limit, $\nu/\omega \to 0$, a resonant singularity appears in the second term in Eq. (1) at the point on the density profile where $\omega_{pe}(x) = \omega$ and, therefore, $\epsilon(x) \to 0$. (By contrast no such resonant singularity appears in the corresponding equation for light polarized normal to the plane of incidence.) In this limit a finite absorption occurs at the singularity. When Eq. (1) is integrated with a linear density gradient such that the density rises linearly from $\omega_{pe} = 0$ at $x = 0$ to $\omega_{pe} = \omega$ at $x = L$, and the connection formulae at the singularity are given only by $\nu > 0$ and $\nu/\omega \to 0$, the power absorption coefficients plotted in Fig. 1 are obtained. The maxima indicate that there is an optimum angle of incidence for absorption. For $k_oL = 10$ this is seen to be at $(k_oL)^{\frac{2}{3}} \sin^2\theta \simeq 0.7$ or $\theta \simeq 23°$. For large L, i.e., weaker density gradients, the optimum angle is smaller, i.e., more nearly normal incidence. Figures 2a, 2b, and 2c show real and imaginary parts of the nonzero components of the solution of Eq. (1) when $k_oL = 10$ and $\theta = 23°$. The phase of the wave, i.e., the choice of real and imaginary parts is taken to be such that B_z is pure real at $x = L$ (Fig. 2a). The absorption is caused by the nonzero E_x wave field, which only occurs when there is non-normal incidence with this polarization, and which drives plasma oscillations in the x direction with frequency ω. At the critical surface where $\omega = \omega_{pe}$, the natural frequency of these plasma oscillations, their amplitude becomes very large, in fact inversely proportional to ν, and as $\nu \to 0$ the collisional energy dissipation smoothly approaches the finite limit plotted in Fig. 1. From Figs. 2a and 2c the x component of the Poynting vector is a step function, finite and constant to the left of

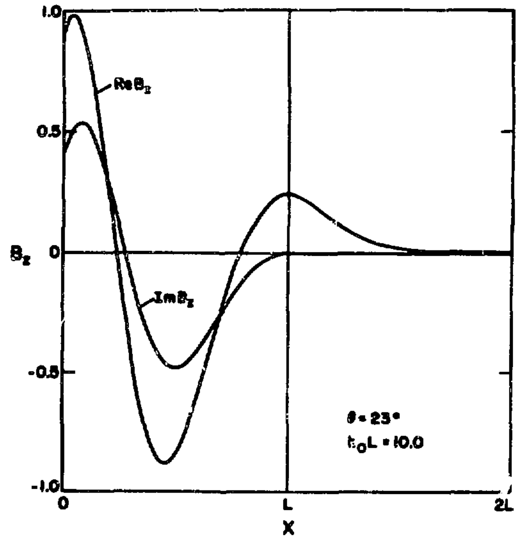

Fig. 2a. B_z vs x for the case $k_oL = 10$ at the optimum angle of $\theta = 23°$ in the limit $\nu/\omega \to 0$.

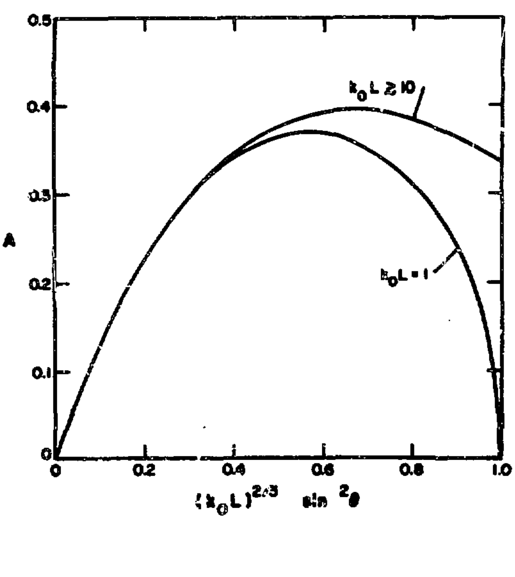

Fig. 1. Rate of energy absorption, A, as a function of angle of incidence, θ, vacuum wave number, k_o, and distance from the front edge to the critical surface, L.

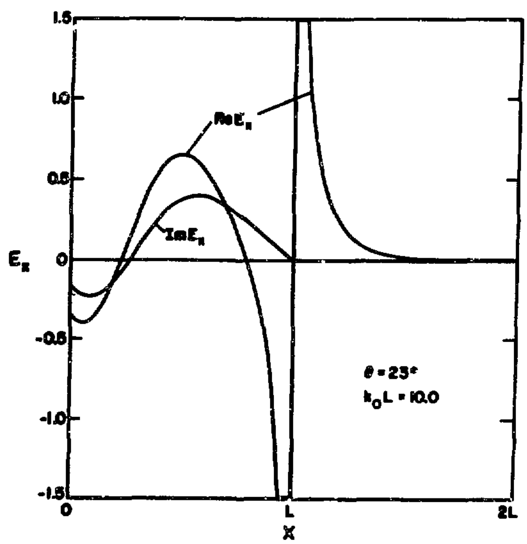

Fig. 2b. E_x vs x for the case $k_oL = 10$ at the optimum angle of $\theta = 23°$ in the limit $\nu/\omega \to 0$.

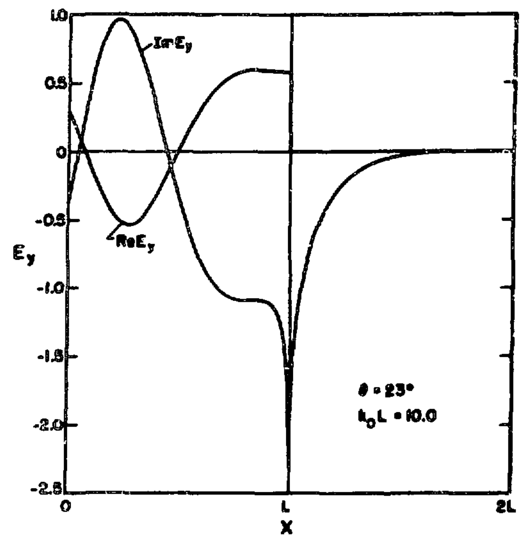

Fig. 2c. E_y vs x for the case $k_0L = 10$ at the optimum angle of $\theta = 23°$ in the limit $\nu/\omega \to 0$.

$x = L$ and zero to the right with ReE_y (Fig. 2c) where ReB_z (Fig. 2a) remains finite. This is consistent with a very large real x component of the electron current, J_x, at $x = L$ which is in phase with, and therefore absorbs energy from the electromagnetic part of ReE_x. (ImE_x is zero at $x = L$, Fig. 2b, except for a delta function there which does not appear explicitly in the calculations and does not contribute directly to the absorption in this approximation.) This part of E_x, which drives the oscillations in the first place and which is nonsingular at $x = L$, is reduced to zero by the changing x projection as $\bar{k}_0$ turns toward normal incidence and is reduced by the increased tunneling distance from the classical turning point where $\omega_{pe}^2/\omega^2 = \cos^2\theta$ to $x = L$ where $\omega_{pe}^2/\omega^2 = 1$ when θ becomes large. Hence there is a maximum absorption at intermediate values of θ, an argument which can be formalized to estimate that the maximum occurs where $(k_0L)^{\frac{2}{3}} \sin^2\theta \simeq (\frac{1}{2})^{\frac{2}{3}}$.

The linear density profile is qualitatively like most of the profiles expected in practice when an initially sharp surface expands a bit into the vacuum during heating, sometimes because of a weak precursor before a short main pulse. Of course the magnitude of the absorption will depend somewhat on the details of the profile. For instance a more nearly flat spot in the profile near the critical surface can enhance the absorption.

Collisional resonant absorption of obliquely incident radiation has been studied previously by the model used above, but without numerical integrations, in the context of microwave propagation in the ionosphere,(1) (also other references contained in Ref. 1). Essentially the same effect seems to be observed in studies of the infrared irradiation of thin metal films.(2)

The preceding linearized treatment implicitly assumes that the amplitude of the x displacements of the electrons which in steady state is

$$\xi(x) = \frac{eE_d}{m[\omega^2 - \omega_{pe}^2(x) - i\nu\omega_0]} \qquad (3)$$

where E_d is the electromagnetic part of E_x referred to above which drives the oscillations, is so small that it can be neglected.

However, for any given amplitude of wave field there is some region around the critical surface where this is not true when $\nu/\omega \to 0$ and where, in fact, the approximate condition for phase space breaking, $|d\xi/dx| > 1$ is satisfied. In this collisionless regime the breaking of the electron plasma waves or oscillations in the resonant region takes the place of collisions in limiting the amplitude of the oscillations and thereby absorbing wave energy. Since in most applications this process only limits the electron oscillations near the critical surface, as does the significant collisional damping when $0 < \nu/\omega \ll 1$, they appear essentially the same in the large and the absorption rates of Fig. 1 can be applied to collisionless cases as well.

In order to reach this understanding of the collisionless resonant absorption, which is quite nonlinear, it was necessary to treat the problem by particle-in-cell numerical simulation.(3) Since the problem is basically two-dimensional (except for a version of the problem which is infinite but <u>not</u> periodic in y), a self-consistent treatment required fully electromagnetic two-dimensional (in x and y) simulations which were done using the method of Appendix B in Ref. 3 with periodicity in y. The results of these two-dimensional simulations, which will be published in a more complete article, show that the following one-dimensional simulation method gives a qualitatively correct picture of the collisionless resonant electron heating in addition to affording higher spatial resolution. An oscillating $E_{dx}(x,t)$ field is arbitrarily imposed, as in Eq. (3) above, with a smooth bell-shaped profile in x centered at x = L and broad enough to extend well on either side of the region where the resonant absorption occurs. The electrons, and the ions if they are mobile, move in x and their resulting charge density is used to compute an additional electrostatic E_x field from Poisson's equation as if the system were independent of y. This E_x determines the motion of the particles. In the dimensionless units of the simulation, Fig. 3, a particle with unit velocity travels a unit distance in a unit time, and the frequency of E_{dx}, which is of course equal to the plasma frequency at the critical surface, is $\omega = 1$, i.e., a period of the driving field is 2π. The maximum amplitude of E_{dx} at x = L is such that a free electron would oscillate with a maximum x velocity, V_x, of one, which is much less that the resonantly enhanced values seen in Fig. 3.

At t = 0, Fig. 3a, the electrons, which are cold, and the ions, which are fixed, have a linear density profile which rises from zero at x = 0 to twice the critical density at x = 2L = 600 with the critical density at x = L = 300. The sinusoidal oscillations of E_{dx} begin at this time and the oscillations build up without breaking until at t = 41 through 43, Figs. 3b and 3c, breaking occurs for the first time. A simple analysis like that of Eq. (3), with transients included instead of $\nu \neq 0$ if one wishes, shows that oscillations on either side of x = L should be 180° out of phase with one

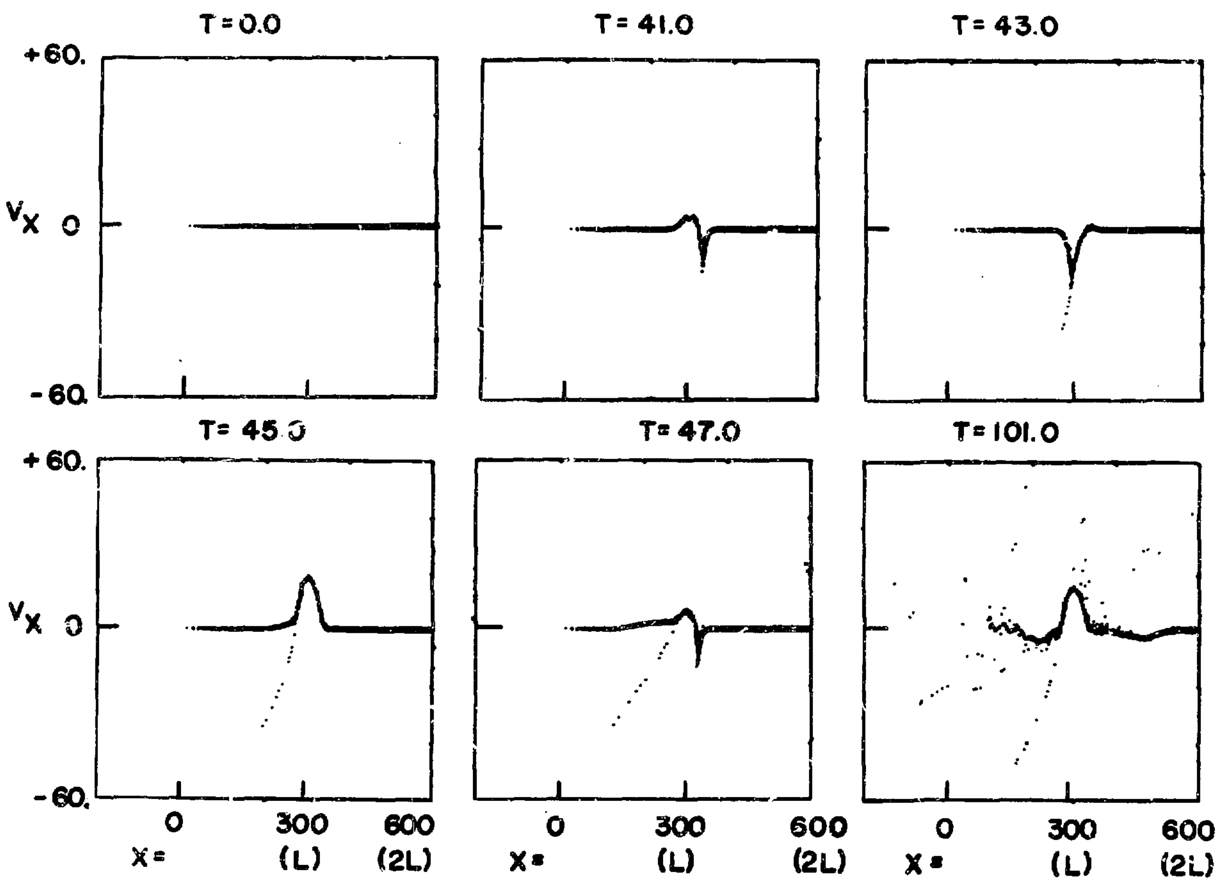

Fig. 3. Electron phase space plot of a one-dimensional simulation of the collisionless absorption. Note the few scattered electrons at large energies in d, e, and f.

another with those very close to x = L being 90° out of phase with both in such a sense that the total wave motion near x = L appears like a sequence of waves growing up on the high density side and moving toward the lower density side followed by a rarefaction-like motion back to the high density side as seen in Fig. 3d at t = 45. Hence, as observed here, the breaking should occur to the left, i.e., toward the vacuum, and not to the right. In Fig. 3e, t = 47, the high energy electrons from the first breaking are moving toward the vacuum where they will be reflected back to the right by a charge separation potential, Fig. 3f. The breaking process at the critical surface is about to repeat as it does on every cycle from then on in about the same way if, as in this code, the hot electrons are absorbed at the right wall and replaced by reemission of cold electrons. The energy is then effectively deposited in the interior of the target by collisionless electron thermal conductivity. Figure 3f shows the situation much later at t = 101. Plainly the heated electrons are much more energetic than they would be with the maximum free electron velocity of $V_x = 1$ and thus constitute a very non-Maxwellian high temperature tail on an otherwise essential cold electron velocity distribution. Figure 4 shows the distribution of ions at t = 200 from an otherwise identical run but with mobile H^+ ions. Electron pressure is causing the front surface ions to blow off with a rather high energy and is pushing ions away from the critical surface, which has the effect of temporarily partially quenching the resonance.

Recent one- and two-dimensional simulations including relativistic particle dynamics have also shown that when the laser wave field is sufficiently intense a significant fraction of the incident energy is imparted to the electrons in a manner similar to that seen above by the oscillating radiation pressure, i.e., the $\bar{V} \times \bar{B}$ force. Here, however, polarization and angle of incidence are not so important and the resulting electron energy distribution shows less of the two-temperature structure seen above.

ACKNOWLEDGEMENTS

This work was first presented at the September 23-27, 1971 Gordon Conference on the Interaction of Laser Light with Matter.

REFERENCES

1. P. Hirsch and J. Shmoys, Radio Science Journal of Research NBS/USNC-URSI, Vol. 69D, No. 4, 521 (1965).

2. M. Skibowski, B. Feuerbacher, W. Steinmann, and R. P. Godwin, Z. für Physik 211, 329 (1968).

3. R. L. Morse and C. W. Nielson, Phys. Fluids 14, 830 (1971).

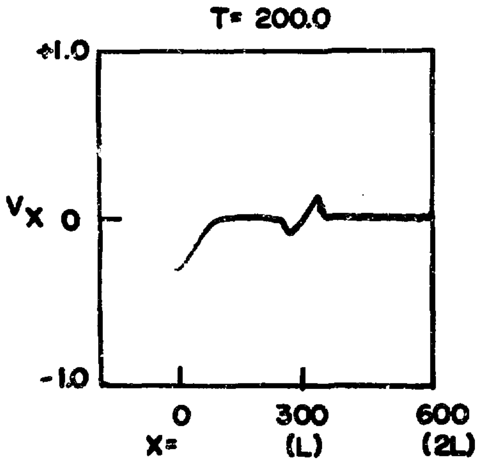

Fig. 4. Phase space plot of H^+ ions.